Quantum anomalous Hall insulator in ionic Rashba lattice of correlated electrons

Marcin M. Wysokiński[1,*] and Wojciech Brzezicki[1,2,†]

[1]*International Research Centre MagTop, Institute of Physics, Polish Academy of Sciences, Aleja Lotników 32/46, PL-02668 Warsaw, Poland*

[2]*Institute of Theoretical Physics, Jagiellonian University, Prof. Stanisława Łojasiewicza 11, PL-30348 Kraków, Poland*

(Received 17 March 2023; accepted 6 July 2023; published 12 July 2023)

In this work, we propose an exactly solvable two-dimensional lattice model of strongly correlated electrons that realizes a quantum anomalous Hall insulator with Chern number $\mathcal{C} = 1$. First, we show that the interplay of ionic potential, Rashba spin-orbit coupling, and Zeeman splitting leads to the appearance of quantum anomalous Hall effect. Next, we calculate in an exact manner the Chern number for the correlated system where electron-electron interactions are introduced in the spirit of the Hatsugai-Kohmoto model using two complementary methods, one relying on the properties of many-body ground state and the other utilizing single-particle Green's function, and subsequently we determine stability regions. By leveraging the presence of inversion symmetry, we find boundaries between topological and trivial phases on the analytical ground. Notably, we show that in the presence of correlations, onset of topological phase is no longer signaled by a spectral gap closing consistently with phenomenon called *first-order topological transition* in literature. We provide a clear microscopic understanding of this inherently many-body feature by pinpointing that the lowest energy excited states in the correlated system are no longer of the single-particle nature and thus, are not captured by a spectral function.

DOI: 10.1103/PhysRevB.108.035121

I. INTRODUCTION

Research on the intersection of topological phases and strongly correlated systems has attracted significant attention in recent years [1]. This is mostly because the description of topological properties of the correlated matter remains an open, though intensively studied [2–4], problem, as most available classifications concern noninteracting systems [5–9].

Apart from rare examples, especially concerning a phenomenon called first-order topological transitions [10–15], usually correlations are taken into account together with nontrivial topology by mapping effects of many-body interactions into the effective single-particle picture possibly encompassing symmetry breaking phases. In that manner the resulting effective Hamiltonian is suitable for topological analysis within the known classifications. Illustrative examples not involving symmetry broken states are, for instance, topological Kondo insulators where the effect of strong correlations is mostly accounted for by renormalization of hybridization gap and up-shift of the atomic level of f electrons [16,17]. On the other hand, a well-known example involving symmetry broken states is the one proposed by Raghu *et al.,* [18] where appearance of topological state, and also opening of the charge gap, is linked to the onset of interaction driven charge density wave.

In the present work we address the problem of interplay between correlations and topology from a different angle [19], which recently gained some attention [20–22]. Namely, we aim to analyze the effect of correlations on a quantum anomalous Hall (QAH) insulator by taking into account only part of the full Hubbard type of interaction in the Hatsugai-Kohmoto (HK) spirit [23], i.e., interaction term local in momentum space, that, when strong enough, leads to the opening of the charge Mott gap that can be analyzed with the exact calculations. In the past such a form of interaction has been used for description of so-called statistical spinliquid [24,25] and its instability toward superconductivity [26]. Moreover, more recently, the same interaction was advocated to be essential when it comes to the understanding of discrete symmetry breaking on a Mott metal to insulator transition [27], as well as properties of high T_c cuprate superconductors [28].

There are several systems realizing or being predicted to realize QAH effect [29–39] whose topological properties derive from the band structure character, specific form of spin-orbit coupling, and magnetic order. Here, we propose yet another model system realizing QAH as a result of interplay between ionic potential, Rashba spin-orbit interaction, and Zeeman splitting. It is promising for potential experimental realization that mentioned ingredients of the model system can be found altogether either in a synthetic version in the optical lattice with engineered spin-orbit coupling [40,41] or in thin layers of ionic insulators doped with magnetic ions.

Our exact analysis of the topological properties of the proposed model in the presence of correlations introduced in HK spirit performed with two complementary techniques, based on exact many-body ground state as well as single particle Green's function [42,43] unveiled that (i) the QAH state, though in narrower a range of parameters than in the uncorrelated case, survives despite high but finite values of

*wysokinski@magtop.ifpan.edu.pl
†brzezicki@magtop.ifpan.edu.pl

interactions and (ii) the spectral gap is not closing at the topological phase transition even for small values of interactions, consistently with the phenomenon called, in literature, *first-order topological phase transition* [11–15]. The latter finding, being a clear manifestation of the inherently many-body nature of the considered system, is directly explained on the microscopic ground. It also constitutes another example [20] where analysis of single-particle Green's function in a correlated system can provide misleading conclusions related to topological properties.

II. MODEL

Our starting point is a single-orbital ionic Rashba model in the presence of Zeeman splitting on the bipartite square lattice:

$$\begin{aligned}\mathcal{H}_0 = &-t\sum_{\langle \mathbf{ij}\rangle\sigma} c^\dagger_{\mathbf{i}\sigma}c_{\mathbf{j}\sigma} + \sum_{\mathbf{i}\sigma}[V(-1)^{\mathbf{i}} + \sigma h - \mu]n_{\mathbf{i}\sigma} \\ &+ \sum_{\langle \mathbf{ij}\rangle}\left(i\alpha(c^\dagger_{\mathbf{i}\uparrow}, c^\dagger_{\mathbf{i}\downarrow})(\mathbf{r_{ij}}\times\boldsymbol{\sigma})_z \begin{pmatrix} c_{\mathbf{j},\uparrow} \\ c_{\mathbf{j},\downarrow}\end{pmatrix} + \text{H.c.}\right),\end{aligned} \tag{1}$$

where t is the nearest-neighbor hopping, V is the strength of the ionic potential, $(-1)^{\mathbf{i}\in A} = 1$ and $(-1)^{\mathbf{i}\in B} = -1$, h Zeeman field, α amplitude of Rashba spin-orbit interaction, $\mathbf{r_{ij}}$ measures the distance between sites $\mathbf{i}$ and $\mathbf{j}$, and $\boldsymbol{\sigma} = \{\sigma_x, \sigma_y, \sigma_z\}$ is vector of Pauli matrices. Hereafter, we set t as an energy unit, i.e., $t = 1$.

After Fourier transformation to the reduced Brillouin zone (RBZ) above model can be cast into the following form:

$$\begin{aligned}\mathcal{H}_0 = &\sum_{\mathbf{k}\in\text{RBZ}} \hat\psi^\dagger_{\mathbf{k}}(\sigma_z\otimes[\Re(g_{\mathbf{k}})\sigma_x + \Im(g_{\mathbf{k}})\sigma_y + \epsilon_{\mathbf{k}}\mathbb{1}] \\ &+ V\sigma_x\otimes\mathbb{1} + h\mathbb{1}\otimes\sigma_z - \mu\mathbb{1}_4)\hat\psi_{\mathbf{k}},\end{aligned} \tag{2}$$

where $g_{\mathbf{k}} = 2\alpha\sin k_y - i2\alpha\sin k_x$, $\epsilon_{\mathbf{k}} = -2t(\cos k_x + \cos k_y)$, and $\hat\psi^\dagger_{\mathbf{k}} = \{c^\dagger_{\mathbf{k},\uparrow}, c^\dagger_{\mathbf{k},\downarrow}, c^\dagger_{\mathbf{k}+\mathbf{Q},\uparrow}, c^\dagger_{\mathbf{k}+\mathbf{Q},\downarrow}\}$ with $Q = \{\pi, \pi\}$.

At this stage we enrich the single particle Hamiltonian $\mathcal{H}_0$ with many-body correlations introduced in the Hatsugai-Kohmoto spirit [23],

$$\mathcal{H} = \mathcal{H}_0 + \sum_{\mathbf{k}\in\text{RBZ}} U(n_{\mathbf{k}\uparrow}n_{\mathbf{k}\downarrow} + n_{\mathbf{k}+\mathbf{Q}\uparrow}n_{\mathbf{k}+\mathbf{Q}\downarrow}). \tag{3}$$

Considered a many-body model due to local in momentum form of the interaction is exactly solvable. Throughout the whole paper we set $\mu = U/2$, what ensure half-filling independently of the other parameters.

As a side remark we note that HK interaction can be seen as a part of the Hubbard interaction,

$$U\sum_{\mathbf{i}} n_{\mathbf{i}\uparrow}n_{\mathbf{i}\downarrow} = \frac{U}{N}\sum_{\mathbf{k},\mathbf{p},\mathbf{q}} c^\dagger_{\mathbf{k}+\mathbf{p}-\mathbf{q}\uparrow}c^\dagger_{\mathbf{q}\downarrow}c_{\mathbf{p}\uparrow}c_{\mathbf{k}\downarrow}$$

for $\mathbf{k} = \mathbf{p} = \mathbf{q}$, that is responsible for splitting between Hubbard bands and eventually opening a Mott gap once the interactions are strong enough [23,27,28]. At the same time, we underline that the presence of the splitting between Hubbard bands by HK interaction for arbitrarily small amplitudes U has no analogy in the system with Hubbard interaction where Fermi-liquid behavior is expected.

III. TOPOLOGY OF MANY-BODY GROUNDSTATE

A. Chern number of the groundstate

Our Hamiltonian can be efficiently expressed in RBZ as

$$\mathcal{H} = \sum_{\mathbf{k}\in\text{RBZ}}\sum_{n\in\{0-4\}} |\hat\alpha^n_{\mathbf{k}}\rangle\hat{\mathcal{H}}^n_{\mathbf{k}}\langle\hat\alpha^n_{\mathbf{k}}|, \tag{4}$$

where $|\hat\alpha^n_{\mathbf{k}}\rangle$ are vectors of Fock basestates in which Hamiltonian $\mathcal{H}$ can be exactly diagonalized, and where n stands for the number of particles described by these states. Explicitly, we define $|\hat\alpha^n_{\mathbf{k}}\rangle$ as

$$\begin{aligned}|\hat\alpha^0_{\mathbf{k}}\rangle &= \{|0_{\mathbf{k}}; 0_{\mathbf{k}+\mathbf{Q}}\rangle\}, \\ |\hat\alpha^1_{\mathbf{k}}\rangle &= \{|\uparrow; 0\rangle, |\downarrow; 0\rangle, |0; \uparrow\rangle, |0; \downarrow\rangle\}, \\ |\hat\alpha^2_{\mathbf{k}}\rangle &= \{|\uparrow\downarrow; 0\rangle, |0; \uparrow\downarrow\rangle, |\downarrow; \downarrow\rangle, |\downarrow; \uparrow\rangle, |\uparrow; \uparrow\rangle, |\uparrow; \downarrow\rangle\}, \\ |\hat\alpha^3_{\mathbf{k}}\rangle &= \{|\uparrow\downarrow; \uparrow\rangle, |\uparrow\downarrow; \downarrow\rangle, |\uparrow; \uparrow\downarrow\rangle, |\downarrow; \uparrow\downarrow\rangle\}, \\ |\hat\alpha^4_{\mathbf{k}}\rangle &= \{|\uparrow\downarrow; \uparrow\downarrow\rangle\}.\end{aligned} \tag{5}$$

On the other hand, Hamiltonian sectors $\hat{\mathcal{H}}^n_{\mathbf{k}}$ in the above base apart from trivial $\mathcal{H}^0_{\mathbf{k}} = \mathcal{H}^4_{\mathbf{k}} = 0$ are defined as

$$\begin{aligned}\hat{\mathcal{H}}^1_{\mathbf{k}} &= \sigma_z\otimes(\epsilon_{\mathbf{k}}\mathbb{1}_2 + \Re(g_{\mathbf{k}})\sigma_x + \Im(g_{\mathbf{k}})\sigma_y) + h\mathbb{1}_2\otimes\sigma_z \\ &\quad + V\sigma_x\otimes\mathbb{1}_2 - \frac{U}{2}\mathbb{1}_4, \\ \hat{\mathcal{H}}^3_{\mathbf{k}} &= \sigma_z\otimes(\epsilon_{\mathbf{k}}\mathbb{1}_2 - \Re(g_{\mathbf{k}})\sigma_x - \Im(g_{\mathbf{k}})\sigma_y) + h\mathbb{1}_2\otimes\sigma_z \\ &\quad - V\sigma_x\otimes\mathbb{1}_2 - \frac{U}{2}\mathbb{1}_4,\end{aligned} \tag{6}$$

and

$$\hat{\mathcal{H}}^2_{\mathbf{k}} = \begin{pmatrix} 2\epsilon_{\mathbf{k}} & 0 & 0 & -V & 0 & V \\ 0 & -2\epsilon_{\mathbf{k}} & 0 & -V & 0 & V \\ 0 & 0 & -2h-U & -g_{\mathbf{k}} & 0 & g_{\mathbf{k}} \\ -V & -V & -g^*_{\mathbf{k}} & -U & g_{\mathbf{k}} & 0 \\ 0 & 0 & 0 & g^*_{\mathbf{k}} & 2h-U & -g^*_{\mathbf{k}} \\ V & V & g^*_{\mathbf{k}} & 0 & -g_{\mathbf{k}} & -U \end{pmatrix}. \tag{7}$$

For the reason that the chemical potential $\mu = U/2$ sets the filling in our system to two not only on average, but at each $\mathbf{k}$ in RBZ, the global many-body ground state is the ground state $|\psi_g(\mathbf{k})\rangle$ of $\hat{\mathcal{H}}^2_{\mathbf{k}}$. Therefore, here we calculate the Chern number of the whole system as the one corresponding to $|\psi_g(\mathbf{k})\rangle$, i.e.,

$$\begin{aligned}\mathcal{C} = \frac{1}{2\pi i}\int_{\mathbf{k}\in\text{RBZ}} d^2\mathbf{k}\,\big(&\partial_{k_x}\langle\psi_g(\mathbf{k})|\partial_{k_y}|\psi_g(\mathbf{k})\rangle \\ &- \partial_{k_y}\langle\psi_g(\mathbf{k})|\partial_{k_x}|\psi_g(k)\rangle\big).\end{aligned} \tag{8}$$

The above topological invariant is directly linked to the anomalous Hall conductance, as shown in Ref. [44]. In Fig. 1 we show phase diagrams obtained by direct integration with the use of discretization of RBZ [45]. We note that although the presence of the Rashba spin-orbit coupling mixing spin channels is critical for the onset of the QAH phase, the topological phase boundaries do not change when the value of

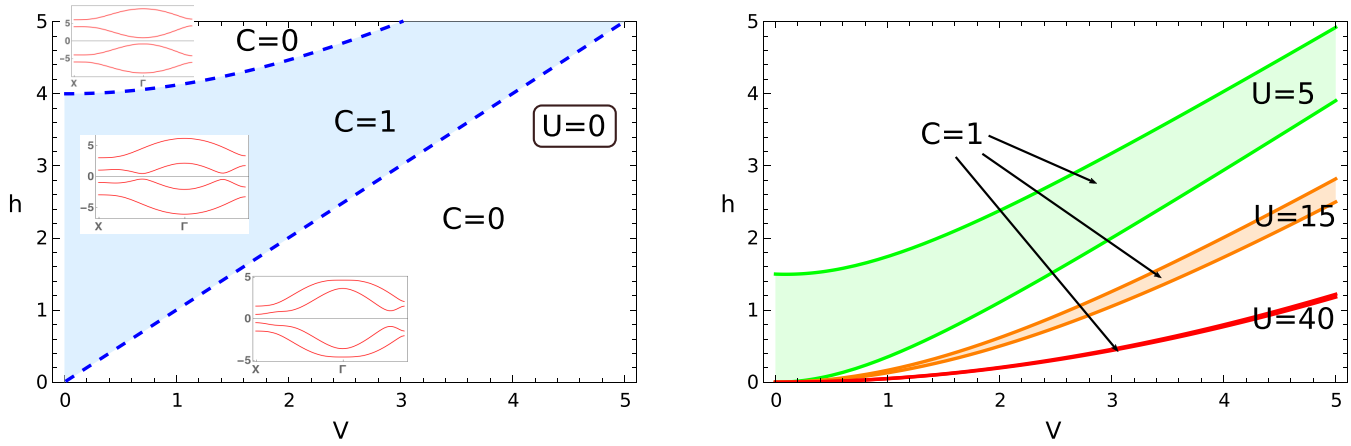

FIG. 1. Topological phase diagrams ("C" on the plots denotes Chern number) on $V-h$ plane for (left panel) uncorrelated system and (right panel) correlated systems characterized with selected values of interaction amplitude U. Phase boundaries marked with dashed lines denote standard topological phase transition, while those with solid lines denote topological phase transitions at which spectral gap doesn't close (see Sec. IV). On the left panel we have included an exemplary band structure for each of the phases along the RBZ high-symmetry path (cf. inset of Fig. 2). The specific parameters are $\alpha = 0.5$, $V = 1$ and $h \in \{0.5, 2, 5\}$ for the bottom, middle, and top inset, respectively.

α is varied. We rigorously support this statement in the next subsection. Nevertheless, for all numerical calculations we set $\alpha = 0.5$.

Furthermore, as it can be seen in Fig. 1, even for extremely large values of interaction amplitude, the Chern insulator survives, though in a very restricted region that asymptotically reduces to a line. In the following we analyze that behavior on the analytical ground.

B. Parity eigenvalues analysis

Analysis of $\hat{\mathcal{H}}^2_{\mathbf{k}}$ at time reversal invariant momenta (TRIM) $\mathbf{k}^*_i$, due to presence of inversion symmetry, can be useful in determination of borders between topological and trivial phases, provided that they differ by the parity of the Chern number. Here this seems sufficient as our numerical analysis unveils the presence of only one type of topological phase (cf. Fig. 1) with $\mathcal{C} = 1$.

First, we find eigenstates $|n_{\mathbf{k}^*_i}\rangle$ and eigenvalues $E_{n\mathbf{k}^*_i}$ of $\hat{\mathcal{H}}^2_{\mathbf{k}^*_i}$, where TRIM in RBZ can be chosen as $\mathbf{k}^*_i \in \{\Gamma, X\}$. Two lowest energy states are $|1_{\mathbf{k}^*_i}\rangle \equiv |\downarrow,\downarrow\rangle$ with the eigenvalue $E_{1\mathbf{k}^*_i} = -U - 2h$ and $|2_{\mathbf{k}^*_i}\rangle$, with eigenvalue $E_{2\mathbf{k}^*_i}$; the latter being the lowest eigenvalue of the matrix

$$\begin{pmatrix} 0 & \sqrt{2}\epsilon_{\mathbf{k}^*_i}u_- & \sqrt{2}\epsilon_{\mathbf{k}^*_i}u_+ \\ \sqrt{2}\epsilon_{\mathbf{k}^*_i}u_- & \frac{-U-\sqrt{U^2+16V^2}}{2} & 0 \\ \sqrt{2}\epsilon_{\mathbf{k}^*_i}u_+ & 0 & \frac{-U+\sqrt{U^2+16V^2}}{2} \end{pmatrix}, \tag{9}$$

$$u_\pm = \sqrt{1 \pm \frac{U}{\sqrt{U^2+16V^2}}},$$

that is simply one of the blocks from block-diagonal form of $\hat{\mathcal{H}}^2_{\mathbf{k}^*_i}$ obtained with a suitable unitary transformation and spanned by $\{|\uparrow\downarrow, 0\rangle, |0, \uparrow\downarrow\rangle, \frac{1}{\sqrt{2}}(|\uparrow,\downarrow\rangle - |\downarrow,\uparrow\rangle)\}$ Fock states.

At TRIM states, $|n_{\mathbf{k}^*_i}\rangle$ are also eigenstates with eigenvalues η_n of parity operator

$$P = \begin{pmatrix} 1 & 0 & 0 & 0 & 0 & 0 \\ 0 & 1 & 0 & 0 & 0 & 0 \\ 0 & 0 & -1 & 0 & 0 & 0 \\ 0 & 0 & 0 & 1 & 0 & 0 \\ 0 & 0 & 0 & 0 & -1 & 0 \\ 0 & 0 & 0 & 0 & 0 & 1 \end{pmatrix}, \tag{10}$$

as $P\hat{\mathcal{H}}^2_{\mathbf{k}}P = \hat{\mathcal{H}}^2_{-\mathbf{k}}$ implies that $[P, \hat{\mathcal{H}}^2_{\mathbf{k}^*}] = 0$. At both TRIM we have that $\eta_1 = -1$ and $\eta_2 = 1$. Formally, by defining

$$(-1)^\nu = \prod_{i\in\Gamma,X} \operatorname{sgn}\left[E_{1k^*_i} - E_{2k^*_i}\right], \tag{11}$$

$\nu = 0$ signals trivial insulator and $\nu = 1$ topologically nontrivial state. In other words, phase transition between trivial and nontrivial topological states takes place when ground state and first excited state, having opposite parity, interchange. Note that, although presence of Rashba spin orbit entails presence of states with opposite parity, its amplitude does not enter Eq. (11). This proves our statement from the previous subsection that boundaries between topological and trivial phases do not depend on Rashba spin-orbit amplitude.

Leveraging supplementary topological invariant (11) allowing for straightforward discrimination between topological and trivial phases in the following we analyze specific phase boundaries displayed in Fig. 1.

First, we examine conditions for transition from the trivial insulator to the Chern insulator with increasing Zeeman splitting h, i.e., from the "bottom"—cf. Fig. 1. At critical Zeeman splitting, which we denote h_b, two lowest energy levels at TRIM X cross. At this momenta these energy levels are found exactly: $E_{1X} = -U - 2h$ and $E_{2X} = -\frac{1}{2}(U + \sqrt{U^2+16V^2})$. Critical Zeeman field at which bottom topological transition takes place can be obtained from a condition that $E_{1X} = E_{2X}$ and reads

$$h_b(V,U) = \tfrac{1}{4}(\sqrt{U^2+16V^2} - U). \tag{12}$$

Second, topological phase transition into the same Chern insulator phase but with decreasing h (from the "top"—cf. Fig. 1) takes place at critical $h = h_t$ when $E_{1\Gamma} = E_{2\Gamma}$, i.e., is associated with crossing between lowest lying energy levels at Γ TRIM. Here, $E_{2\Gamma}$ can be obtained exactly only for the $U = 0$ case, for which we find $E_{2\Gamma} = -2\sqrt{V^2 + \epsilon_\Gamma^2}$ [lowest eigenvalue of (9)], where $\epsilon_\Gamma \equiv \epsilon_{\mathbf{k}^*_\Gamma}$. Thus, critical Zeeman splitting for the "top" topological phase transition in the uncorrelated case reads $h_t(V, U = 0) = \sqrt{V^2 + \epsilon_\Gamma^2}$. On the other hand, in the opposite limit (i.e., large interaction limit, $\sqrt{2}\epsilon_\Gamma/U \ll 1$), we resort to the second order perturbation theory when obtaining $E_{2\Gamma}$ and we find

$$E_{2\Gamma} \simeq E_{2X} - \frac{(\sqrt{U^2 + 16V^2} - U)(2\epsilon_\Gamma)^2}{\sqrt{U^2 + 16V^2}(\sqrt{U^2 + 16V^2} + U)}. \tag{13}$$

Consequently, approximate critical Zeeman splitting for the "top" topological phase transition in the strong interaction limit reads

$$h_t(V, U \gg \sqrt{2}\epsilon_\Gamma) = h_b(V, U) + \frac{(\sqrt{U^2 + 16V^2} - U)2\epsilon_\Gamma^2}{\sqrt{U^2 + 16V^2}(\sqrt{U^2 + 16V^2} + U)}. \tag{14}$$

As a result, the region on the $V - h$ plane where the Chern insulator with $\mathcal{C} = 1$ is realized, lies between boundaries set by $h_b(U, V)$ and (if U is sufficiently large) $h_t(U, V)$, and only asymptotically vanish when $U \to \infty$, while for large but finite U forms a sharp edge (cf. Fig. 1).

IV. SINGLE PARTICLE GREEN'S FUNCTION PROPERTIES

Knowledge of the exact ground state wave function of the considered system is a necessary factor enabling for the analysis presented in the previous section. Nevertheless, in generic situations with more realistic many-body interactions the system properties are usually captured at the level of single particle Green's function. Therefore, topological invariant defined through single-particle Green's function [43] is considered as the default one when it comes to description of the topological properties of the many-body system. However, it has been recently proven [20] that it needs to be treated with care as it can give false positive topological properties even if the system is trivial. For that reason, in the following we analyze topological and spectral properties of the considered system at the level of single-particle Green's function and carefully compare findings with the precise analysis of the many-body ground state.

A. Spectral function and absence of gap closing

In the previous section we have shown that the topological phase transition is signaled by crossing between ground state and first excited state, both many-body Fock states, that takes place at one of the time-reversal invariant momenta. As we are going to analyze in this section, this usual and expected behavior, due to the presence of correlations, does not entail closure of the spectral gap.

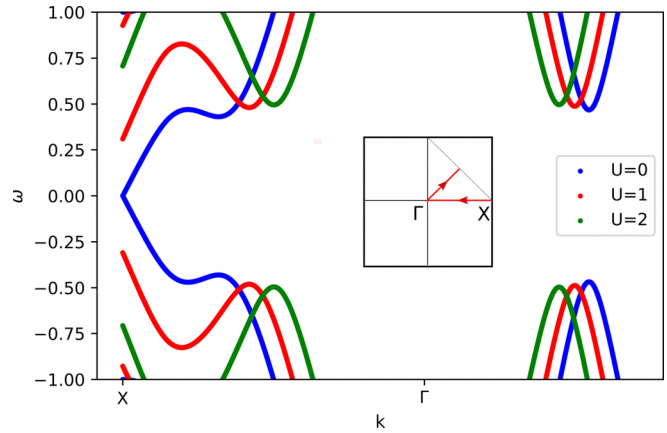

FIG. 2. Plot of the spectral function in the vicinity of the Fermi level along a high symmetry path (cf. inset) for values of $h = h_b$, i.e., at the topological phase transition. Note the lack of a gap closing in the spectral function for nonzero interaction strength. The spectral weight for bands visible in the plot is close to one.

We first define

$$\hat{\mathcal{H}}_\mathbf{k} = \bigoplus_{n=0}^{4} \hat{\mathcal{H}}^n_\mathbf{k} \quad \text{and} \quad |\hat{\alpha}_\mathbf{k}\rangle = \bigoplus_{n=0}^{4} |\hat{\alpha}^n_\mathbf{k}\rangle. \tag{15}$$

Now, we can find unitary transformation $T_\mathbf{k}$, such that $T_\mathbf{k}^\dagger \hat{\mathcal{H}}_\mathbf{k} T_\mathbf{k} = \hat{E}_\mathbf{k}$ is diagonal. As a result, we can obtain spectral function as

$$A(\mathbf{k}, \omega) = \frac{1}{\pi} \Im \operatorname{Tr}[\hat{G}_\mathbf{k}(\omega - i\delta)], \tag{16}$$

where Matsubara Green's function reads

$$\hat{G}_\mathbf{k}(i\omega) = \begin{pmatrix} G^{1,1}_{\uparrow,\uparrow} & G^{1,1}_{\uparrow,\downarrow} & G^{1,2}_{\uparrow,\uparrow} & G^{1,2}_{\uparrow,\downarrow} \\ G^{1,1}_{\downarrow,\uparrow} & G^{1,1}_{\downarrow,\downarrow} & G^{1,2}_{\downarrow,\uparrow} & G^{1,2}_{\downarrow,\downarrow} \\ G^{2,1}_{\uparrow,\uparrow} & G^{2,1}_{\uparrow,\downarrow} & G^{2,2}_{\uparrow,\uparrow} & G^{2,2}_{\uparrow,\downarrow} \\ G^{2,1}_{\downarrow,\uparrow} & G^{2,1}_{\downarrow,\downarrow} & G^{2,2}_{\downarrow,\uparrow} & G^{2,2}_{\downarrow,\downarrow} \end{pmatrix} \tag{17}$$

with matrix elements obtained from Lehmann representation as

$$G^{n,n'}_{\sigma,\sigma'}(i\omega) = \sum_m \left[\frac{\langle 0|c_{n,\sigma}|m\rangle \langle m|c^\dagger_{n',\sigma'}|0\rangle}{i\omega - (E_m - E_0)} + \frac{\langle m|c_{n,\sigma}|0\rangle \langle 0|c^\dagger_{n',\sigma'}|m\rangle}{i\omega + (E_m - E_0)} \right]. \tag{18}$$

In the above $|m\rangle$ are the exact eigenvectors ($|0\rangle$ being ground state) of $\hat{\mathcal{H}}_\mathbf{k}$ with eigenvalues E_m, and $c_{1\sigma} \equiv c_{\mathbf{k}\sigma}$ and $c_{2\sigma} \equiv c_{\mathbf{k}+\mathbf{Q}\sigma}$.

In Fig. 2 we show spectral function around the Fermi level for parameters providing "bottom" topological phase transition, i.e., for $h = h_b(V, U)$, for three selected cases: uncorrelated $U = 0$, and correlated $U = 1$ and $U = 2$ ones. It is evident that the spectral gap closes at the topological phase transition only for uncorrelated states. Such observation is consistent with a phenomenon called first-order topological transition found in other many-body topological systems with more realistic, usually Hubbard-type, interactions [10–15] for

which it has been also found that correlations can entail absence of the spectral gap closing on the topological transition. Here, relying on the previous analysis of the exact ground state, we shall simply explain microscopic reasons for such a situation and briefly elaborate on the misleading notion coined for this phenomenon.

Spectral function is a single-particle property of the system and, as such, tells us how the injected electron behaves in our system. That means that the spectral function holds information about processes that involve excitation that change the number of particles in the system. On the other hand, as our analysis of the exact many-body ground state unveils, the first excited state in the presence of interactions does not involve a change of electron number. Therefore, spectral function is unable to capture crossing of the ground state and first excited state that signals regular continuous topological phase transition without any feature suggesting first-order character.

In this light, given that spectral function already can provide misleading signatures on the character of topological transition, there is a natural question whether single particle Green's function in a correlated state beyond Fermi liquid theory still contains enough information to calculate correct boundaries of topological phase. In the next subsection we affirmatively answer this question.

B. Topological invariant from Green's function

Here we calculate the topological invariant of our system, following the approach in Ref. [43]. In general words, in this method one can treat the inverse of Green's function for zero frequency as an effective low-energy single-particle Hamiltonian,

$$H^{\text{eff}}_{\mathbf{k}} = -G_{\mathbf{k}}(0)^{-1}. \tag{19}$$

In such a situation, determination of the topological invariant of the system reduces to analysis of H^{eff} [which is Hermitian—cf. Eq. (17)].

We first find eigenvectors and eigenvalues of effective Hamiltonian

$$H^{\text{eff}}_{\mathbf{k}}|n(\mathbf{k})\rangle = \mu_n(\mathbf{k})|n(\mathbf{k})\rangle. \tag{20}$$

Then the many-body topological invariant can be obtained as

$$\tilde{\mathcal{C}} = \frac{1}{2\pi}\int_{\text{RBZ}} d^2k\left(\partial_{k_x}\mathcal{A}_y - \partial_{k_y}\mathcal{A}_x\right), \tag{21}$$

where $\mathcal{A}_i = -i\sum_{n(\mu_n<0)}\langle n(\mathbf{k})|\partial_{k_i}|n(\mathbf{k})\rangle$.

We numerically confirm that the above approach provides the same topological phase borders as the approach utilizing true many-body ground states presented in Sec. III and in principle $\mathcal{C} = \tilde{\mathcal{C}}$. We note that, although here spectral function is unable to visualize inversion between ground state and first excited state, single-particle Green's function holds correct information of the system's topology.

In the following we shall analyze more deep properties of the low-energy effective Hamiltonian. We found that the topological phase transition is again not associated with the bulk gap closing, as it is demonstrated in Fig. 3, and clearly the system develops singularity at X TRIM. To understand it in more detail, in Fig. 4 we plot bands around TRIM X just before and after transition, which confirms the expectation

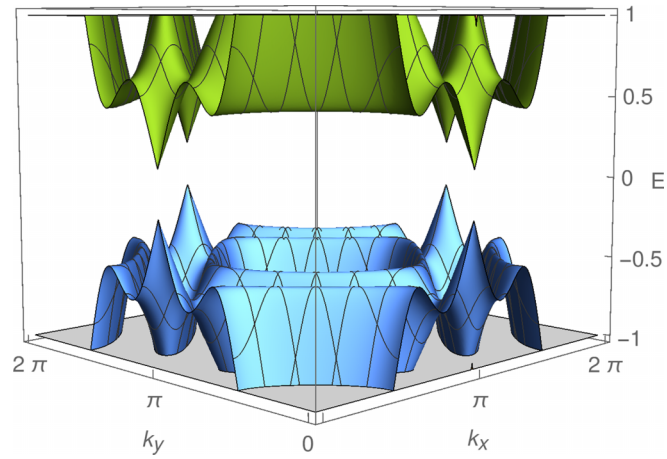

FIG. 3. Eigenenergies of effective low-energy single particle Hamiltonian around Fermi level for parameters providing "bottom" topological phase transition, i.e. $h = h_b$ [cf. Eq. (12)]. Note the absence of the gap closing.

that the phase transition takes place through the discontinuous jump of eigenenergies at X. Particularly this feature has been responsible for calling such observation *topological phase transition with first-order character* in the first place [11].

This brings us to a following question: if topological and trivial phases are not separated by gap closing, is the topological phase inside the bulk separated from the trivial "outside"? To resolve this issue, in Fig. 5 we plot bands of $H^{\text{eff}}_{\mathbf{k}}$, but with the open boundaries along the y direction, and we obtain a rather standard scenario. Namely, that edge states are not gapped and clearly connect bands from below the gap with those from above, and their number per one edge agrees with the Chern number.

C. Properties of H^{eff} at TRIM

In this section we shall again leverage inversion symmetry as a good tool for determining phase transition between trivial and topological phases [42] with an odd Chern number. We start our analysis by finding the parity operator for the full

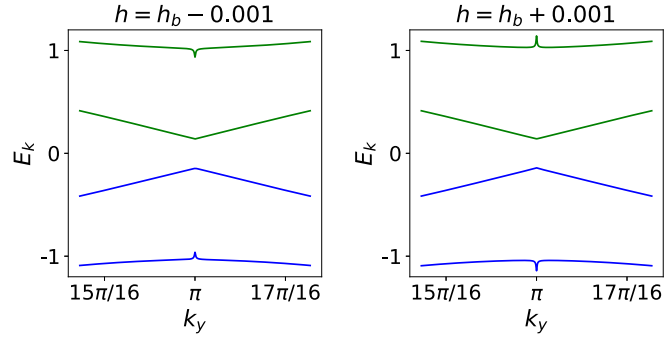

FIG. 4. Bands of $H^{\text{eff}}_{\mathbf{k}}$ around TRIM X i.e. for $k_x = 0$ (left panel) for trivial phase ($h < h_b$) just before transition and (right panel) for topological phase ($h > h_b$) just after the transition. At the transition bands are characterized by a discontinuous jump at TRIM X.

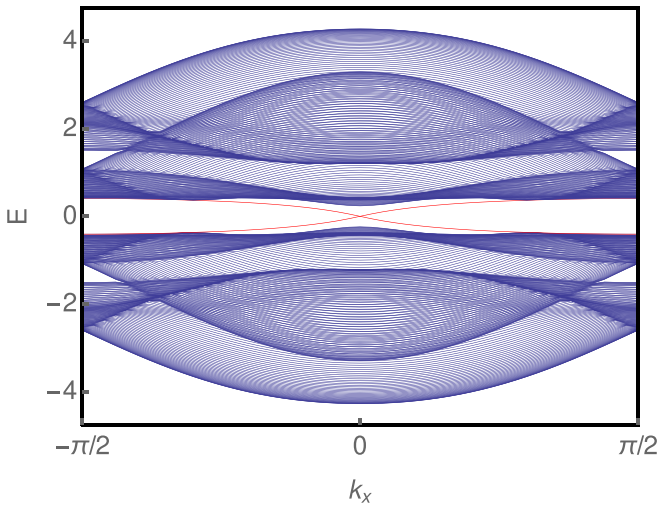

FIG. 5. Bands of $H^{\text{eff}}_{\mathbf{k}}$ with open boundary conditions in the y direction in the topological phase. Edge states are clearly visible. The parametrs are $U = V = 0.5$ and $h = h_b + 0.1$.

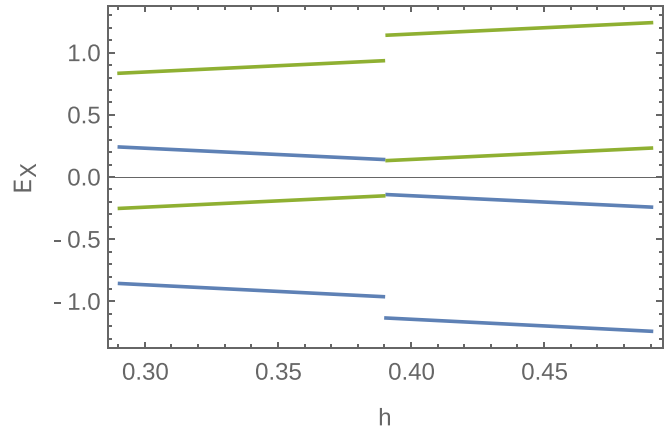

FIG. 6. Evolution of eigenenergies of $H^{\text{eff}}_{\mathbf{k}}$ at TRIM X across the topological phase transition with increasing h. Color denotes different parities of the eigenstates. The topological phase transition takes place through the singularity instead of energy level crossing. Parameters for the plot are $U = V = 0.5$.

Green's function,

$$\mathcal{P} = \begin{pmatrix} 1 & 0 & 0 & 0 \\ 0 & -1 & 0 & 0 \\ 0 & 0 & 1 & 0 \\ 0 & 0 & 0 & -1 \end{pmatrix}, \tag{22}$$

i.e., $\mathcal{P}\hat{G}_{\mathbf{k}}(i\omega_m)\mathcal{P} = \hat{G}_{-\mathbf{k}}(i\omega_m)$. The form of operator $\mathcal{P}$ follows from the symmetry of the Rashba coupling in $\mathcal{H}$. Following the approach presented in Refs. [42,43] we note that zero-frequency single-particle Green's function at TRIMs is Hermitian, commutes with the parity operator, and, specifically for our situation, reduces to

$$\hat{G}_{\mathbf{k}_i^*}(0) = \begin{pmatrix} G^{1,1}_{\mathbf{k}_i^*\uparrow}(0) & 0 & G^{1,2}_{\mathbf{k}_i^*\uparrow}(0) & 0 \\ 0 & G^{1,1}_{\mathbf{k}_i^*\downarrow}(0) & 0 & G^{1,2}_{\mathbf{k}_i^*\downarrow}(0) \\ G^{2,1}_{\mathbf{k}_i^*\uparrow}(0) & 0 & G^{2,2}_{\mathbf{k}_i^*\uparrow}(0) & 0 \\ 0 & G^{2,1}_{\mathbf{k}_i^*\downarrow}(0) & 0 & G^{2,2}_{\mathbf{k}_i^*\downarrow}(0) \end{pmatrix}. \tag{23}$$

Note that we can diagonalize above Green's function with a transformation that leaves the parity operator intact. Transformed and subsequently inverted, Green's function defines effective Hamiltonian at TRIM

$$H^{\text{eff}}_{\mathbf{k}_i^*} = \begin{pmatrix} -\mu_{\mathbf{k}_i^*\uparrow+} & 0 & 0 & 0 \\ 0 & -\mu_{\mathbf{k}_i^*\downarrow+} & 0 & 0 \\ 0 & 0 & -\mu_{\mathbf{k}_i^*\uparrow-} & 0 \\ 0 & 0 & 0 & -\mu_{\mathbf{k}_i^*\downarrow-} \end{pmatrix}, \tag{24}$$

where

$$(\mu_{\mathbf{k}_i^*\sigma\pm})^{-1} = \frac{G^{1,1}_{\sigma\mathbf{k}^*} + G^{2,2}_{\sigma\mathbf{k}^*}}{2} \pm \sqrt{\left(\frac{G^{1,1}_{\sigma\mathbf{k}^*} - G^{2,2}_{\sigma\mathbf{k}^*}}{2}\right)^2 + \left|G^{1,2}_{\sigma\mathbf{k}^*}\right|^2} \tag{25}$$

that still commutes with a parity operator Eq. (22), and therefore both operators have common eigenvectors, i.e.,

$$\begin{aligned} H^{\text{eff}}_{\mathbf{k}^*}|\sigma,\pm,\mathbf{k}^*\rangle &= -\mu_{\sigma,\pm,\mathbf{k}^*}|\sigma,\pm,\mathbf{k}^*\rangle \\ \mathcal{P}|\sigma,\pm,\mathbf{k}^*\rangle &= \eta_{\sigma,\mathbf{k}^*}|\sigma,\pm,\mathbf{k}^*\rangle. \end{aligned} \tag{26}$$

Because of the inversion symmetry [42] we can define invariant ν by

$$(-1)^{\nu} \equiv \prod_{\mathbf{k}^*} \prod_{\{\sigma,\pm\}\in \text{R}-\text{zero}} \eta^{1/2}_{\sigma,\mathbf{k}^*}, \tag{27}$$

where R − zero is defined by eigenstates $|\sigma,\pm\rangle$ with negative eigenvalue $-\mu_{\sigma,\pm} < 0$. As a result, we find that the topological phase transition is signaled when invariant ν changes between zero and one, i.e., when eigenvalues for states with different parities change sign at TRIM. In Fig. 6 we plot eigenenergies $\mu_{\sigma,\pm}$ for increasing field h across the topological phase transition at $h = h_b$ and we found, peculiar for the single particle picture, discontinuous jump of eigenenergies at the topological phase transition, associated with a change of parities of states with positive energies. Such behavior can be understood on the following grounds. Although, at the topological phase transition, the ground state energy remains continuous the state itself changes vastly due to the level crossing with the first excited state within the $|\hat{\alpha}^2_{\mathbf{k}}\rangle$ manifold. This makes the spectrum of the single particle excitations discontinuous as it is visible in Fig. 6.

V. SUMMARY AND CONCLUSIONS

In the present work we have proposed the model in which the interplay between ionic potential, Zeeman splitting, and Rashba spin-orbit interaction realizes quantum anomalous Hall state. In our opinion, the model has an advantage of being potentially realizable experimentally. In future works we are going to explore its potential to govern underlying physics of thin layers of semiconductors having rocksalt structure and negligible internal spin-orbit coupling, epitaxially grown on the substrate ensuring presence of Rashba interaction due to lack of spatial inversion, and doped with magnetic ions providing sizable Zeeman splitting.

Moreover, we have studied the influence of the many-body interaction, introduced in the Hatsugai-Kohmoto spirit [23], on the stability of the topological phase by two complementary techniques leveraging the closed form of the ground state

and Green's function approach. Interestingly, in the presence of correlations we have found that topological phase transition accompanied by expected crossing between ground state and first excited state at the same time is characterized with the absence of a gap closing in the spectral function. The latter feature has been, in light of our results, misleadingly called *first order topological transition*. We explain the absence of spectral gap closing at the topological transition by referring to the many-body nature of lowest energy excited states. To analyze this feature further, by considering the inverse of zero frequency single-particle Green's function as an effective low-energy Hamiltonian, we demonstrated that topological phase transition takes place through a band discontinuity at the time reversal invariant momenta. Thus, our work constitutes another example [20] where analysis of single-particle Green's function in a correlated system can provide misleading conclusions related to topological properties.

ACKNOWLEDGMENTS

The work is supported by the Foundation for Polish Science through the International Research Agendas program cofinanced by the European Union within the Smart Growth Operational Programme. W.B. acknowledges support by Narodowe Centrum Nauki (NCN, National Science Centre, Poland) Project No. 2019/34/E/ST3/00404.

[1] S. Rachel, Interacting topological insulators: A review, Rep. Prog. Phys. **81**, 116501 (2018).
[2] E. M. Stoudenmire, J. Alicea, O. A. Starykh, and M. P. A. Fisher, Interaction effects in topological superconducting wires supporting Majorana fermions, Phys. Rev. B **84**, 014503 (2011).
[3] M. Hohenadler and F. F. Assaad, Correlation effects in two-dimensional topological insulators, J. Phys.: Condens. Matter **25**, 143201 (2013).
[4] A. Więckowski, M. M. Maśka, and M. Mierzejewski, Identification of Majorana Modes in Interacting Systems by Local Integrals of Motion, Phys. Rev. Lett. **120**, 040504 (2018).
[5] A. Altland and M. R. Zirnbauer, Nonstandard symmetry classes in mesoscopic normal-superconducting hybrid structures, Phys. Rev. B **55**, 1142 (1997).
[6] C.-K. Chiu, H. Yao, and S. Ryu, Classification of topological insulators and superconductors in the presence of reflection symmetry, Phys. Rev. B **88**, 075142 (2013).
[7] C.-K. Chiu and A. P. Schnyder, Classification of reflection-symmetry-protected topological semimetals and nodal superconductors, Phys. Rev. B **90**, 205136 (2014).
[8] K. Shiozaki and M. Sato, Topology of crystalline insulators and superconductors, Phys. Rev. B **90**, 165114 (2014).
[9] K. Shiozaki, M. Sato, and K. Gomi, Topology of nonsymmorphic crystalline insulators and superconductors, Phys. Rev. B **93**, 195413 (2016).
[10] J. C. Budich, B. Trauzettel, and G. Sangiovanni, Fluctuation-driven topological Hund insulators, Phys. Rev. B **87**, 235104 (2013).
[11] A. Amaricci, J. C. Budich, M. Capone, B. Trauzettel, and G. Sangiovanni, First-Order Character and Observable Signatures of Topological Quantum Phase Transitions, Phys. Rev. Lett. **114**, 185701 (2015).
[12] A. Amaricci, J. C. Budich, M. Capone, B. Trauzettel, and G. Sangiovanni, Strong correlation effects on topological quantum phase transitions in three dimensions, Phys. Rev. B **93**, 235112 (2016).
[13] J. Imriška, L. Wang, and M. Troyer, First-order topological phase transition of the Haldane-Hubbard model, Phys. Rev. B **94**, 035109 (2016).
[14] B. Roy, P. Goswami, and J. D. Sau, Continuous and discontinuous topological quantum phase transitions, Phys. Rev. B **94**, 041101(R) (2016).
[15] S. Barbarino, G. Sangiovanni, and J. C. Budich, First-order topological quantum phase transition in a strongly correlated ladder, Phys. Rev. B **99**, 075158 (2019).
[16] M. Dzero, K. Sun, V. Galitski, and P. Coleman, Topological Kondo Insulators, Phys. Rev. Lett. **104**, 106408 (2010).
[17] M. M. Wysokiński and M. Fabrizio, Many-body breakdown of indirect gap in topological Kondo insulators, Phys. Rev. B **94**, 121102(R) (2016).
[18] S. Raghu, X.-L. Qi, C. Honerkamp, and S.-C. Zhang, Topological Mott Insulators, Phys. Rev. Lett. **100**, 156401 (2008).
[19] T. Morimoto and N. Nagaosa, Weyl Mott insulator, Sci. Rep. **6**, 19853 (2016).
[20] M.-F. Yang, Manifestation of topological behaviors in interacting weyl systems: One-body versus two-body correlations, Phys. Rev. B **100**, 245137 (2019).
[21] P. Mai, B. E. Feldman, and P. W. Phillips, Topological Mott insulator at quarter filling in the interacting Haldane model, Phys. Rev. Res. **5**, 013162 (2023).
[22] P. Mai, J. Zhao, B. E. Feldman, and P. W. Phillips, 1/4 is the new 1/2: Interaction-induced quantum anomalous and spin Hall Mott insulators, arXiv:2210.11486.
[23] Y. Hatsugai and M. Kohmoto, Exactly solvable model of correlated lattice electrons in any dimensions, J. Phys. Soc. Jpn. **61**, 2056 (1992).
[24] K. Byczuk and J. Spałek, Statistical properties and statistical interaction for particles with spin: The Hubbard model in one dimension and a statistical spin liquid, Phys. Rev. B **50**, 11403 (1994).
[25] K. Byczuk and J. Spałek, Universality classes, statistical exclusion principle, and properties of interacting fermions, Phys. Rev. B **51**, 7934 (1995).
[26] K. Byczuk and J. Spałek, Application of statistical spin liquid concept to high temperature superconductivity, Acta Phys. Pol. A **85**, 337 (1994).
[27] E. W. Huang, G. L. Nave, and P. W. Phillips, Discrete symmetry breaking defines the Mott quartic fixed point, Nat. Phys. **18**, 511 (2022).
[28] P. W. Phillips, L. Yeo, and E. W. Huang, Exact theory for superconductivity in a doped Mott insulator, Nat. Phys. **16**, 1175 (2020).
[29] C.-Z. Chang, J. Zhang, X. Feng, J. Shen, Z. Zhang, M. Guo, K. Li, Y. Ou, P. Wei, L.-L. Wang, Z.-Q. Ji, Y. Feng, S. Ji, X. Chen, J. Jia, X. Dai, Z. Fang, S.-C. Zhang, K. He, Y. Wang *et al.*,

Experimental observation of the quantum anomalous Hall effect in a magnetic topological insulator, Science **340**, 167 (2013).

[30] C.-Z. Chang, W. Zhao, D. Y. Kim, H. Zhang, B. A. Assaf, D. Heiman, S.-C. Zhang, C. Liu, M. H. W. Chan, and J. S. Moodera, High-precision realization of robust quantum anomalous Hall state in a hard ferromagnetic topological insulator, Nat. Mater. **14**, 473 (2015).

[31] A. L. Sharpe, E. J. Fox, A. W. Barnard, J. Finney, K. Watanabe, T. Taniguchi, M. A. Kastner, and D. Goldhaber-Gordon, Emergent ferromagnetism near three-quarters filling in twisted bilayer graphene, Science **365**, 605 (2019).

[32] Y. Deng, Y. Yu, M. Z. Shi, Z. Guo, Z. Xu, J. Wang, X. H. Chen, and Y. Zhang, Quantum anomalous Hall effect in intrinsic magnetic topological insulator $MnBi_2Te_4$, Science **367**, 895 (2020).

[33] M. Serlin, C. L. Tschirhart, H. Polshyn, Y. Zhang, J. Zhu, K. Watanabe, T. Taniguchi, L. Balents, and A. F. Young, Intrinsic quantized anomalous Hall effect in a moiré heterostructure, Science **367**, 900 (2020).

[34] Y. Satake, J. Shiogai, G. P. Mazur, S. Kimura, S. Awaji, K. Fujiwara, T. Nojima, K. Nomura, S. Souma, T. Sato, T. Dietl, and A. Tsukazaki, Magnetic-field-induced topological phase transition in Fe-doped $(Bi,Sb)_2Se_3$ heterostructures, Phys. Rev. Mater. **4**, 044202 (2020).

[35] K. M. Fijalkowski, M. Hartl, M. Winnerlein, P. Mandal, S. Schreyeck, K. Brunner, C. Gould, and L. W. Molenkamp, Coexistence of Surface and Bulk Ferromagnetism Mimics Skyrmion Hall Effect in a Topological Insulator, Phys. Rev. X **10**, 011012 (2020).

[36] N. Pournaghavi, M. F. Islam, R. Islam, C. Autieri, T. Dietl, and C. M. Canali, Realization of the Chern-insulator and axion-insulator phases in antiferromagnetic $MnTe/Bi_2(Se,Te)_3/MnTe$ heterostructures, Phys. Rev. B **103**, 195308 (2021).

[37] T. Li, S. Jiang, B. Shen, Y. Zhang, L. Li, Z. Tao, T. Devakul, K. Watanabe, T. Taniguchi, L. Fu, J. Shan, and K. F. Mak, Quantum anomalous Hall effect from intertwined moiré bands, Nature (London) **600**, 641 (2021).

[38] G. Hussain, A. Fakhredine, R. Islam, R. M. Sattigeri, C. Autieri, and G. Cuono, Correlation-driven topological transition in Janus two-dimensional vanadates, Materials **16**, 1649 (2023).

[39] C.-Z. Chang, C.-X. Liu, and A. H. MacDonald, Colloquium: Quantum anomalous Hall effect, Rev. Mod. Phys. **95**, 011002 (2023).

[40] Z. Meng, L. Huang, P. Peng, D. Li, L. Chen, Y. Xu, C. Zhang, P. Wang, and J. Zhang, Experimental Observation of a Topological Band Gap Opening in Ultracold Fermi Gases with Two-Dimensional Spin-Orbit Coupling, Phys. Rev. Lett. **117**, 235304 (2016).

[41] L. Huang, Z. Meng, P. Wang, P. Peng, S.-L. Zhang, L. Chen, D. Li, Q. Zhou, and J. Zhang, Experimental realization of two-dimensional synthetic spin-orbit coupling in ultracold Fermi gases, Nat. Phys. **12**, 540 (2016).

[42] Z. Wang, X.-L. Qi, and S.-C. Zhang, Topological invariants for interacting topological insulators with inversion symmetry, Phys. Rev. B **85**, 165126 (2012).

[43] Z. Wang and S.-C. Zhang, Simplified Topological Invariants for Interacting Insulators, Phys. Rev. X **2**, 031008 (2012).

[44] Q. Niu, D. J. Thouless, and Y.-S. Wu, Quantized hall conductance as a topological invariant, Phys. Rev. B **31**, 3372 (1985).

[45] T. Fukui, Y. Hatsugai, and H. Suzuki, Chern numbers in discretized Brillouin zone: Efficient method of computing (spin) Hall conductances, J. Phys. Soc. Jpn. **74**, 1674 (2005).